Porous Media Flow on Locally Refined Grids

R. H. J. Gmelig Meyling, W. A. Mulder, and G. H. Schmidt

Royal/Dutch Shell, Exploration and Production Laboratory,
P.O. Box 60, NL-2280AB Rijswijk, The Netherlands

Abstract

A numerical method is described for the simulation of miscible and immiscible fluid flow in hydrocarbon reservoirs. A flexible gridding technique introduces both static and dynamic local grid refinement for multiple space dimensions. Operator splitting and defect correction are used to deal separately with elliptic and hyperbolic problems. The elliptic equations are discretised by mixed finite elements and solved by multigrid. Mixed finite elements provide an accurate representation of the flows and allow for a good connection with the hyperbolic equations. The method of characteristics is used for the hyperbolic problems, eliminating numerical diffusion almost completely. Nonlinear phenomena are treated by suitable Riemann solvers.

1 Introduction

The simulation of fluid flow through porous media is of crucial importance in hydrocarbon reservoir engineering. This paper presents some aspects of the research on numerical methods for porous media flow at the Royal Dutch/Shell Laboratory.

A number of features of the computational method will be described. These features must be compatible so that they can be combined into a solution method both for miscible and immiscible fluid displacement. The starting point of the computations is the set of equations for fluids consisting of N (chemical) components in M phases, with N and M arbitrary. A review of the modelling aspects of these equations can be found e.g. in Allen et al. (1988).

The first feature concerns the gridding. The highly varying length scales occurring in large-scale reservoir simulation give rise to a lasting demand for *flexible gridding*. The flow near wells and geological heterogeneities needs locally high accuracy. A fine grid moving along with the solution is required to avoid numerical diffusion at sharp (saturation) fronts and to compute their position accurately. The literature on dynamic gridding distinguishes methods with moving gridpoints (see e.g. Miller (1986)) and methods based on dynamic refinement

in a grid with static points (see Ewing (1988) for an excellent review). We use the latter method, since we wish to perform computations in up to three space dimensions. Moreover, we want a uniform approach for one, two, and three space dimensions. More details of this gridding technique can be found in Schmidt (1990).

The second feature concerns the discretisation. Many of the equations are discretised by using *mixed finite elements.* This means that the fluid fluxes are primary variables, instead of eliminating them and using only scalar fields (such as pressures) as primary variables. Many computational techniques for porous medium flow are based on this discretisation (see e.g. Chavent et al. (1984), Russell and Wheeler (1983)). These authors all refer back to Raviart and Thomas (1977). We use this discretisation, not only because of accuracy arguments, but also because it is suitable for introducing local refinement and for imbedding the use of characteristics into the method. For the combination of mixed finite elements and characteristics see also Douglas and Yirang (1988).

The third feature concerns the solution of large systems of coupled equations. *Multigrid* is a technique to solve very large systems and is used in many areas of computational fluid dynamics, see e.g. Wesseling (1990). The role of multigrid in our approach is to solve symmetric systems only. The technique is specially adapted to the mixed finite elements; for details see Schmidt and Jacobs (1988).

The last feature is the use of the *method of characteristics* to solve hyperbolic systems of equations. As compared to standard finite differences and finite elements, this introduces almost no numerical diffusion and permits very large time steps. It is common in reservoir simulation to use characteristics to solve the two-phase Buckley-Leverett equations in one-dimensional problems. In this paper, characteristics are used to solve hyperbolic equations in up to three space dimensions. Riemann solvers enable us to treat nonlinear effects and to maintain a large time step (see Gmelig Meyling (1990)).

The plan of this paper is as follows. Section 2 describes the general equations for porous media flow. The solution techniques are presented in Sect. 3, whereas Sect. 4 outlines the adaptive gridding. Although the numerical techniques are quite general, they have so far only be applied to *two*-phase flow. Numerical examples for the immiscible flow of oil and water are presented in Sect. 5.

2 Equations for porous media flow

For the flow of fluid consisting of N (chemical) components in M phases through a porous medium we have the following relations.

First, there is a conservation law for each component (chemical reactions are not considered in this paper):

$$\frac{\partial a_n}{\partial t} + \nabla \cdot \mathbf{u}_n = q_n\,, \quad n = 1, \ldots, N \tag{1}$$

Second, the flux of each phase is given by Darcy's law:

$$\mathbf{v}_m = -\lambda_m \mathcal{K} \left(\nabla p_m - \rho_m \mathbf{g}\right), \quad m = 1, \ldots, M \tag{2}$$

Third, the equations are coupled by a number of phenomena:

- The components are convected in the phases, which implies that the $\mathbf{v}_m$ occur (usually linearly) in expressions for the $\mathbf{u}_n$.
- The pressures p_m depend on the concentrations a_n.

A closed set of equations is obtained by imposing the proper initial- and boundary conditions, so that a unique solution may be expected. The features of such a full set of equations depend strongly on the specific fluids and the properties of the porous medium, but usually a combination of elliptic, parabolic and hyperbolic behaviour is observed.

3 Solution techniques

Observation of the flow through porous media leads to distinction into (i) fields which have a strong spatial coupling (e.g., pressure and total fluid flow), and (ii) fields which have (in finite time-intervals) limited ranges of mutual dependence (e.g., saturations and concentrations). *A good solution technique should incorporate this distinction.* For a broad class of problems in porous media flow, we can reduce the full set of PDE's to a basic elliptic set of PDE's and a basic hyperbolic set of PDE's, by using operator splitting and defect correction. Parabolic behaviour is accomodated by the elliptic equations, by virtue of implicit discretisation of the time derivative. The details of the operator splitting and defect correction depend strongly on the specific application and are beyond the scope of this paper. The two basic sets of equations are:

The *basic elliptic set of equations*:

$$cp + \nabla . \mathbf{u} = q \,, \tag{3}$$

$$\nabla p + \mathbf{W}\,\mathbf{u} = \mathbf{g} \,, \tag{4}$$

to be solved for the scalar p and the vector $\mathbf{u}$, as functions of the space co-ordinate vector $\mathbf{x}$. The scalar c usually represents a compressibility coefficient divided by the time step. The tensor $\mathbf{W}$ usually represents the inverse of a permeability or diffusion tensor.

The *basic hyperbolic set of equations*:

$$\frac{\partial a_n}{\partial t} + \nabla . \mathbf{f}_n(a_1, \ldots, a_N, \mathbf{x}) = q_n(a_1, \ldots, a_N, \mathbf{x}), \quad n = 1, \ldots, N, \tag{5}$$

to be solved for the concentrations $a_1, \ldots, a_N$ as functions of time t and space co-ordinate $\mathbf{x}$.

The solution of the full set of equations consists of a series of time steps. Each time step of size Δt requires solution of the two basic sets at least once. Efficiency and accuracy are obtained by selecting appropriate techniques for each of the basic sets.

3.1 Multigrid for elliptic equations

The technique we use for solving (3–4) has been reported on e.g. in Schmidt and Jacobs (1988). Here we mention just some of its features, mainly in relation with its role in the scheme for solution of the full set of equations.

- The equations (3–4) are discretised using *mixed finite elements*. This implies a direct approximation of $\mathbf{u}$, instead of eliminating it by equation (4). We expect that the elliptic equations are thus better imbedded in the solution scheme of the full set of equations. The coupling of (3–4) with the other (hyperbolic) equations is primarily through $\mathbf{u}$.
- We use mixed finite elements of *lowest order*, i.e., a piecewise constant representation for p and a piecewise linear representation for the components of $\mathbf{u}$ (see Raviart and Thomas (1977)). The coefficients in (3–4) change rapidly (even over one or a couple of meshwidths) in the usual applications, which makes higher order approximation less suitable. When very rapid changes in the coefficients occur (e.g., at fronts, near wells, and near geological discontinuities), accuracy is improved by means of local grid refinement.
- The discrete equations are solved by multigrid as described for 2D problems in Schmidt and Jacobs (1988). Our current codes work on 1D, 2D and 3D grids with similar performance. The role of multigrid is strictly limited to the solution of the *symmetric* system (3–4). All non-symmetric terms are dealt with in the hyperbolic equations by means of suitable operator splitting and/or defect correction.
- The multigrid process solves the discretisation of (3) always with machine-accuracy, while the accuracy of solving (4) depends on the number of multigrid iterations made. This is in accordance with the usual physical interpretation of these equations: equation (3) represents fluid conservation (i.e., *kinematics*), and equation (4) represents a law of fluid *dynamics*. The coefficients in the laws of fluid dynamics (e.g., permeability and diffusion) are known with a relatively low accuracy.

3.2 Method of characteristics for hyperbolic equations

We can discern, in principle at least, two methods to solve (5). The first method is to discretize all derivatives by finite elements or finite differences. This introduces considerable numerical diffusion and/or the time step is severely restricted by stability constraints of the *Courant-Friedrich-Lewy* type. A survey of these computational difficulties can be found in Ewing (1983). In the second method one rewrites the PDE's (5) as a set of ordinary differential equations and one solves these ODE's by appropriate techniques. This is known as the *method of characteristics*. Minimal numerical diffusion and large time steps are advantages of the second method. Hence, whenever (5) can be rewritten as a system of ODE's, one should use the second method.

Both methods can be applied on the locally refined grids to be introduced in the next section. Especially the second method profits from the high resolu-

tion given by these grids. This paper reports recent developments of the second method.

For a broad and certainly important class of flow problems in porous media the hyperbolic set of equations can be written as:

$$\frac{\partial a_n}{\partial t} + \nabla \cdot (f_n(a_1, \ldots, a_N)\mathbf{u}(\mathbf{x})) = q_n(a_1, \ldots, a_N, \mathbf{x}), \quad n = 1, \ldots, N \qquad (6)$$

with initial condition $a_n(\mathbf{x}, t = 0) = a_n^0(\mathbf{x})$ for $n = 1, \ldots, N$. Equation (6) is to be solved for a_n, $n = 1, \ldots, N$ as functions of t and $\mathbf{x}$. Recall that these equations hold during one step in the time-stepping scheme as given above. The *total fluid velocity* $\mathbf{u}$ is defined as the sum of the individual component velocities. In each time step the flow $\mathbf{u}$ is computed at least once from the elliptic system (3–4). The representation of $\mathbf{u}$ by mixed finite elements is favourable (apart from accuracy) for the integration scheme to be given below. From now on, we assume that $\mathbf{u}(\mathbf{x})$ is given.

The problem (6) is in N_d space dimensions. It can be reduced to a sequence of *one-dimensional* initial value problems of the form:

$$\frac{\partial a_n}{\partial t} + \frac{\partial}{\partial \xi} f_n(a_1, \ldots, a_N) = q_n(a_1, \ldots, a_N)\,, \qquad (7)$$

$$a_n(\xi, t = 0) = a_n^0(\xi), \quad n = 1, \ldots, N \qquad (8)$$

along *streamlines*. The streamlines are trajectories in $\mathbf{x}$-space defined by the system of ODE's:

$$\frac{d\mathbf{x}}{d\xi} = \mathbf{u}(\mathbf{x}). \qquad (9)$$

Here the parameter ξ runs along streamlines in the direction of flow. If we replace $\mathbf{u}$ by its mixed finite element representation, the system (9) can be solved analytically block-by-block (see Gmelig Meyling (1990)).

Taking account of the piecewise constant representation of a_n, $n = 1, \ldots, N$ with respect to grid blocks turns the system (7–8) into a sequence of *Riemann problems*:

$$\frac{\partial a_n}{\partial t} + \frac{\partial}{\partial \xi} f_n(a_1, \ldots, a_N) = q_n(a_1, \ldots, a_N)\,, \; n = 1, \ldots, N \qquad (10)$$

$$a_n(\xi, t = 0) = \begin{cases} a_{n,i} & , \quad \text{for } \xi < \xi_i \\ a_{n,i+1} & , \quad \text{for } \xi > \xi_i \end{cases} \qquad (11)$$

The Riemann problem is a classical problem in the theory of hyperbolic equations (Lax (1973)). Its initial condition consists of two constant states to the left and right respectively of a discontinuity, which is located here at position ξ_i. The solution of the Riemann problem is formed by the two constant states separated by smooth segments (*rarefaction waves*) and discontinuities (*shocks*). The discontinuities must be constrained by the *Rankine-Hugoniot jump conditions* and *entropy conditions*, which ensure physical correctness of the shocks.

Riemann solvers form the basic building-blocks of our numerical method for solving the system (7–8). A large time step can be maintained only if interactions between waves and shocks belonging to *different* Riemann problems are fully taken into account. Such large-time-step methods have been proposed by Holden et al. (1988) and Leveque (1982). Smooth waves are here represented by a sequence of (small) discontinuities. Whenever two or more discontinuities coalesce, they are merged into one (new) discontinuity for which the Riemann problem is again solved. Since the entire algorithm operates only on discontinuities, there is (almost) no numerical diffusion.

It remains to describe the solution procedure for individual Riemann problems. For the case of *two-phase flow* (e.g., water and oil), equation (10–11) reduces to a *scalar* hyperbolic problem:

$$\frac{\partial s}{\partial t} + \frac{\partial}{\partial \xi} f(s) = q(s) \tag{12}$$

subject to the initial condition:

$$s(\xi, t=0) = \begin{cases} s_i & , \quad \text{for } \xi < \xi_i \\ s_{i+1} & , \quad \text{for } \xi > \xi_i \end{cases} \tag{13}$$

Here s $(0 \leq s \leq 1)$ denotes the *saturation* of one of the phases (e.g., water). Consequently, $1 - s$ is the saturation of the other phase (e.g., oil). In two-phase flow problems, the water *fractional flow function* $f(s)$ usually has an *S-shape*, i.e., it satisfies the conditions:

- $f(0) = 0 \quad , \quad f(1) = 1$;
- $f'(0) = f'(1) = 0$;
- $f(s)$ has precisely one inflection point s_I, i.e., $f'' > 0$ for $0 \leq s < s_I$ and $f'' < 0$ for $s_I < s \leq 1$.

The following simple geometric principle for solving the Riemann problem (12–13) can be found in Concus and Proskurowski (1979):

- If $s_i > s_{i+1}$, then construct the *convex* envelope $h(s)$ of $f(s)$ over the interval $[s_{i+1}, s_i]$;
- If $s_i < s_{i+1}$, then construct the *concave* envelope $h(s)$ of $f(s)$ over the interval $[s_i, s_{i+1}]$.

In those areas, where $f(s) = h(s)$ the solution of (12–13) is a rarefaction wave; in areas with $f(s) \neq h(s)$ the solution is a shock. These techniques have been incorporated in a computer code capable of solving quite general two-phase flow problems in up to three space dimensions.

For *three-phase flow* (involving water, oil and gas) the situation is more complicated. Here the system (7–8) consists of two nonlinear, coupled equations:

$$\frac{\partial s_1}{\partial t} + \frac{\partial}{\partial \xi} f_1(s_1, s_2) = q_1(s_1, s_2) \tag{14}$$

$$\frac{\partial s_2}{\partial t} + \frac{\partial}{\partial \xi} f_2(s_1, s_2) = q_2(s_1, s_2) \tag{15}$$

As unknowns one could select the *saturation* of water (s_1) and gas (s_2). The oil saturation is then defined by $s_3 = 1 - s_1 - s_2$. For certain three-phase flow models however the *Jacobian matrix*:

$$\nabla_{s_1,s_2}\mathbf{f}(s_1,s_2) = \begin{pmatrix} \partial f_1/\partial s_1 & \partial f_1/\partial s_2 \\ \partial f_2/\partial s_1 & \partial f_2/\partial s_2 \end{pmatrix} \tag{16}$$

may have *complex* eigenvalues in some subregions of the saturation space. Bell, Trangenstein and Shubin (1986) have discussed such a model, which is formally *elliptic* rather than hyperbolic. The solution of Riemann problems associated with these equations of *mixed* type is very complicated. Also the method of characteristics can no longer be applied. Many aspects of these *elliptic regions* are not understood. Questions have been raised by many authors concerning the "correctness" of such models for three-phase flow (for example, see Fitt (1990)). Effective solution methods for the Riemann problem of three-phase flow are still under investigation.

4 Gridding

The computational scheme must be able to resolve accurately the moving fronts occuring in porous media flow. We adopt dynamic regridding, which must be computationally inexpensive. Clear coding of the mixed finite element discretisation is obtained when the grid consists of *blocks* on which the scalar quantities are stored, separated by *faces* on which the fluxes are stored. We also want *one* formulation with a dimension N_d that can be chosen as 1, 2, or 3. These considerations led us to the following *hierarchical* grid structure:

- A static regular *base grid* is created by orthogonal "planes" (constant value of a space co-ordinate). The rectangular boxes are called *blocks*. These are separated by rectangular "planes", called *faces*.
- The base grid is refined and unrefined dynamically by the *basic refinement*, which divides a block into 2^{N_d} identical smaller ones.

Our current codes have cartesian co-ordinate systems, but the theory covers also mildly (i.e., without singularities) curvi-linear co-ordinates. For curvi-linear co-ordinates with singularities, such as polar co-ordinates, additional theory is needed at least for the multigrid.

In the examples given in the next section, the grid is refined statically around wells. The dynamic refinement is triggered primarily by saturation. Given a saturation distribution, we refine and coarsen the grid to achieve

$$tol_s/4 < \epsilon_i < tol_s\,, \tag{17}$$

for all blocks i. Here ϵ_i is an indicator for the error in the saturation on block i based on approximations of first- and second-order space-derivatives of the saturation. The tolerance tol_s has a user-specified value. Each time step, the grid is refined iteratively, using saturation values both on the old and new time

level. In each iteration a refinement (to just one level higher) is done if the upper bound in (17) is violated. The number of iterations does not exceed a prescribed maximum number of refinement levels. After refinement, the grid is coarsened in regions where the lower bound in (17) is violated, now using only saturations at the new time level. We can trigger on the total flow field $\mathbf{u}$ also, by introducing appropriate terms in the error indicator ϵ_i.

5 Numerical results

We present a number of numerical examples for two-phase flow, illustrating various aspects of the method. Fluids and rock formation are assumed to be incompressible. In all examples, the absolute permeability of the porous medium is constant. The first is a multi-well problem, the second a convergence study on the size of the time step, and the last a simple three-dimensional example.

5.1 Multi-well problem

The multi-well problem consists of three injection wells and one production well. The dimensionless size of the domain is 3×3. The injectors are located at $(0.9, 0.6)$, $(0.2, 2.8)$, and $(1.8, 2.1)$, with strengths 0.5, 0.2, and 0.3, respectively. Production occurs at $(3.0, 3.0)$. For the mobilities in (2) we take $\lambda_w = s^2$, $\lambda_o = (1-s)^2/2$. Figure 1 shows the solution at 0.67 PVI (*Pore Volume Injected*), after 12 time steps. The result clearly illustrates that numerical diffusion is virtually absent. Such a small amount of cross-flow smearing is difficult to obtain with standard finite difference methods.

5.2 Convergence

Our method should convergence when both the block size and the time step go to zero. Because the grid is adapted dynamically on the basis of a user-specified parameter, we only will consider convergence in terms of a decreasing time step.

The following set of examples is based on a simple inflow/outflow problem. The initial water saturation on the domain $\Omega = [0,1] \times [0,0.5]$ is defined as a hyperbolic tangent in the horizontal direction, which is perturbed by a cosine in the vertical direction. The inflow velocity is specified at the left boundary. At the right outflow boundary, the pressure is prescribed. The upper and lower boundaries are solid walls.

We have mobilities $\lambda_w = s^2$, $\lambda_o = (1-s)^2/2$, $\lambda = \lambda_w + \lambda_o$, and a fractional flow function $f(s) = \lambda_w/\lambda$. The endpoint mobility ratio is $\lambda(1)/\lambda(0) = 2$, which suggests instable displacement. The mobility ratio across the shock however is $\lambda(s_{shock})/\lambda(0) = 0.845$, which implies stable displacement. The latter mobility ratio seems to dominate the stability of the whole process.

Figures 2a–c show the saturation at the same time, but after different numbers of time steps. The results suggest convergence for decreasing time step, and

also show that an acceptable solution can be obtained with relatively few time steps.

We have repeated this exercise for unstable displacement, using different mobilities that result in ratios $\lambda(s_{shock})/\lambda(0) = 2.051$ and $\lambda(1)/\lambda(0) = 7.262$. Figures 3a–c show the solution for an increasing number of time steps. Clearly, no convergence is obtained. The viscous fingering is generated by numerical "noise", which is amplified by the instability of the displacement process. The computations do not converge for $\Delta t \rightarrow 0$, which is in accordance with the ill-posedness of the problem.

A well-posed problem is obtained by adding a small amount of capillary pressure, which acts as a diffusion term and suppresses the instability on the smaller scales. Results are shown in Figs. 4a–c.

These experiments demonstrate that large time steps can be taken if the physical time scale of the problem allows this (no strong dependence of the total flow field on saturation).

5.3 A three-dimensional example

Figure 5 shows a solution of the three-dimensional equivalent of the quarter-five-spot problem. The injection- and production-wells are placed at opposite corners of a unit cube. The result has been obtained at 0.15 PVI in only one time step.

6 Conclusions

- In this paper, a numerical method is presented for computing multi-phase, miscible and immiscible flow through porous media in one, two, and three space dimensions.
- The method uses *adaptive local grid refinement* near wells, geological heterogeneities, and saturation fronts to enhance solution accuracy and to suppress numerical diffusion.
- Symmetric, elliptic equations are discretised by *mixed finite elements* and solved by *multigrid*. This combination provides accurate scalar and vector quantities and is efficient for large-scale reservoir simulation.
- The *method of characteristics* is used to solve hyperbolic systems of equations. The method introduces almost no numerical diffusion. Riemann solvers facilitate the treatment of nonlinearities and permit the use of large time steps.

Acknowledgement

The authors are indebted to the management of Shell Internationale Research Maatschappij BV for permission to publish this paper.

Notation and list of symbols

N_d	dimension $= 1, 2, 3$
$\mathbf{x}$, t	space and time co-ordinates
i , j	number of block, resp. face
n	$= 1, \ldots, N$, (chemical) component
m	$= 1, \ldots, M$, fluid-phase (e.g., water, oil, gas)
a_n , $\mathbf{u}_n$, q_n	concentration, flux, and sourceterm of component n
p_m , $\mathbf{v}_m$, λ_m , ρ_m	pressure, flux, relative mobility and density of phase m
$\mathbf{g}$	acceleration due to gravity
$\mathcal{K}$	(absolute) permeability tensor of porous medium
$\mathbf{u}$	total fluid velocity
ξ	parameter along streamline
s	(water) saturation
$f(s)$	fractional flow function
s_I	inflection point

References

Allen, M. B., Behie, G. A., Trangenstein, J. A.: Multiphase Flow in Porous Media. Springer Verlag (1988).

Bell, J. B., Trangenstein, J. A., Shubin, G. R.: Conservation laws of mixed type describing three-phase flow in porous media. SIAM J. Appl. Math. **46** (1986) 1000–1017.

Chavent, G., Cohen, G., Jaffre, J.: Discontinuous upwinding and mixed finite elements for two-phase flows in reservoir simulation. Computer Methods in Appl. Mechanics and Eng. **47** (1984) 93–118.

Concus, P., Proskurowski, W.: Numerical solution of a nonlinear hyperbolic equation by the random choice method. J. Comput. Phys. **30** (1979) 153–166.

Douglas, J., Yirang, Y.: Numerical simulation of immiscible flow in porous media based on combining the method of characteristics with mixed finite element procedures. In *Numerical Simulation in Oil Recovery*, M.F. Wheeler (ed.), Springer Verlag (1988) 119–131.

Ewing, R. E.: Problems arising in the modeling of processes for hydrocarbon recovery. In *The Mathematics of Reservoir Simulation*, R.E. Ewing (ed.), SIAM, Philadelphia (1983) 3–34.

Ewing, R. E.: Adaptive grid-refinement techniques for treating singularities, heterogeneities and dispersion. In *Numerical Simulation in Oil Recovery*, M.F. Wheeler (ed.), Springer Verlag (1988) 133–149.

Fitt, A. D.: Mixed hyperbolic-elliptic systems in industrial problems. In *Proc. Third European Conf. on Mathematics in Industry*, J. Manley et al. (eds.), Kluwer/Teubner, Stuttgart (1990) 205–214.

Gmelig Meyling, R. H. J.: Numerical methods for solving the nonlinear hyperbolic equations of porous media flow. In *Proceedings of the Third International Conference on Hyperbolic Problems*, Uppsala, June 1990 (to appear).

Holden, H., Holden, L., Hoegh-Krohn, R.: A numerical method for first order nonlinear scalar conservation laws in one dimension. Comp. Math. Appl. **15** (1988) 595–602.

Lax, P. D.: Hyperbolic systems of conservation laws and the mathematical theory of shock waves. Conf. Series in Applied Mathematics **11**, SIAM, Philadelphia (1973).

Leveque, R. J.: Large time step shock-capturing techniques for scalar conservation laws. SIAM J. Numer. Anal. **19** (1982) 1091–1109.

Miller, K.: Recent results on finite element methods with moving nodes. In *Accuracy Estimates and Adaptive Refinements in Finite Element Computations*, I. Babuska et al. (eds.), John Wiley (1986) 325–338.

Raviart, P. A., Thomas, J. M.: A mixed finite element method for second order elliptic problems. In *Mathematical Aspects of the Finite Element Methods*, Lecture Notes in Mathematics Vol. 606 Springer-Verlag (1977) 292–302.

Russell, T. F., Wheeler, M. F.: Finite element and finite difference methods for continuous flows in porous media. In *The Mathematics of Reservoir Simulation*, R.E. Ewing (ed.) (1983) 35–106.

Schmidt, G. H., Jacobs, F. J.: Adaptive local grid refinement and multigrid in numerical reservoir simulation. J. Comput. Phys. **77** (1988) 140–165.

Schmidt, G. H.: A dynamic grid generator and multigrid for numerical fluid dynamics. In *Proceedings of the* 8^{th} *GAMM Conference on Numerical Methods in Fluid Mechanics*, P. Wesseling (ed.), Notes in Numerical Fluid Mechanics Vol. 29, Vieweg, Braunschweig (1990) 493–502.

Wesseling, P.: Multigrid methods in computational fluid dynamics. ZAMM **70** (1990) 337–347.

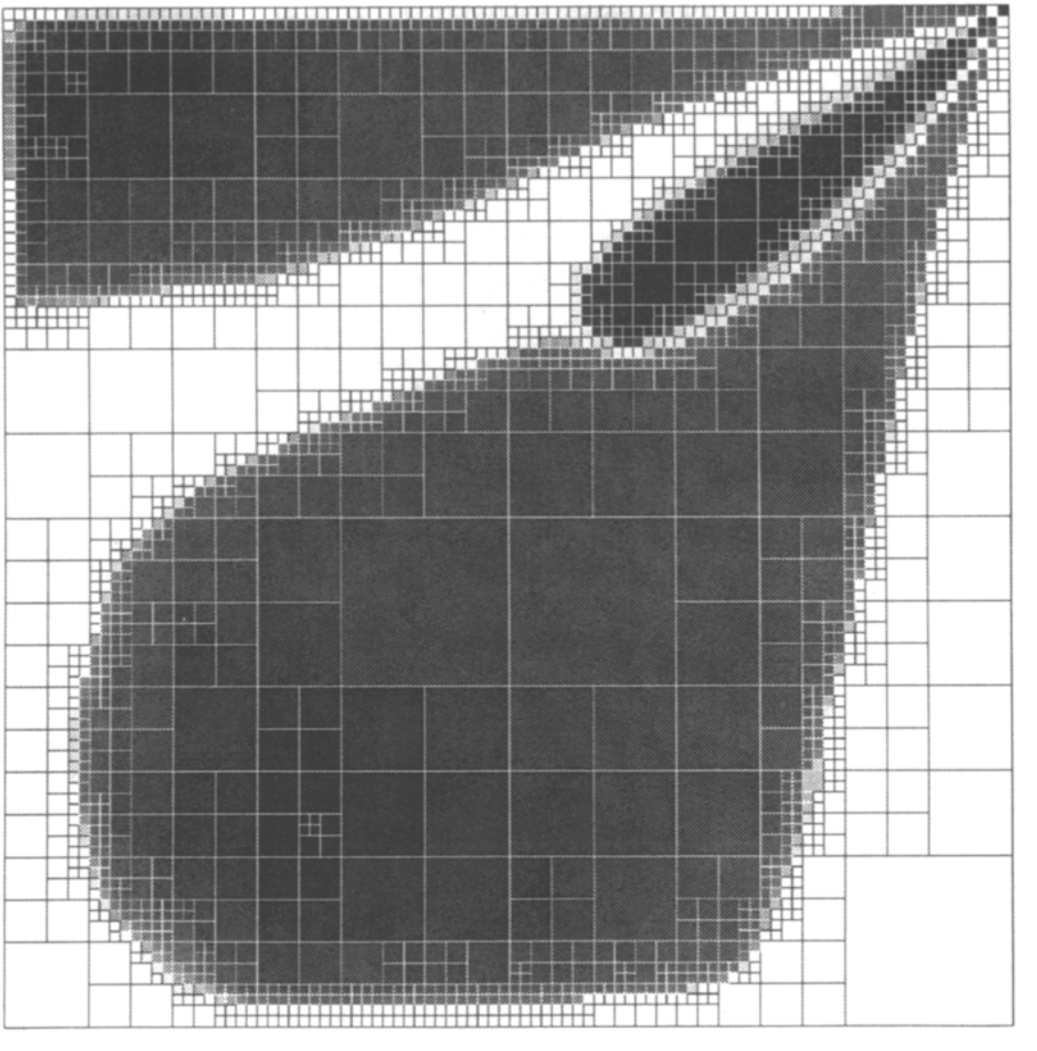

Fig. 1. Solution of the multi-well problem at 0.67 PVI using 12 time steps. Darker halftones correspond to higher water saturations.

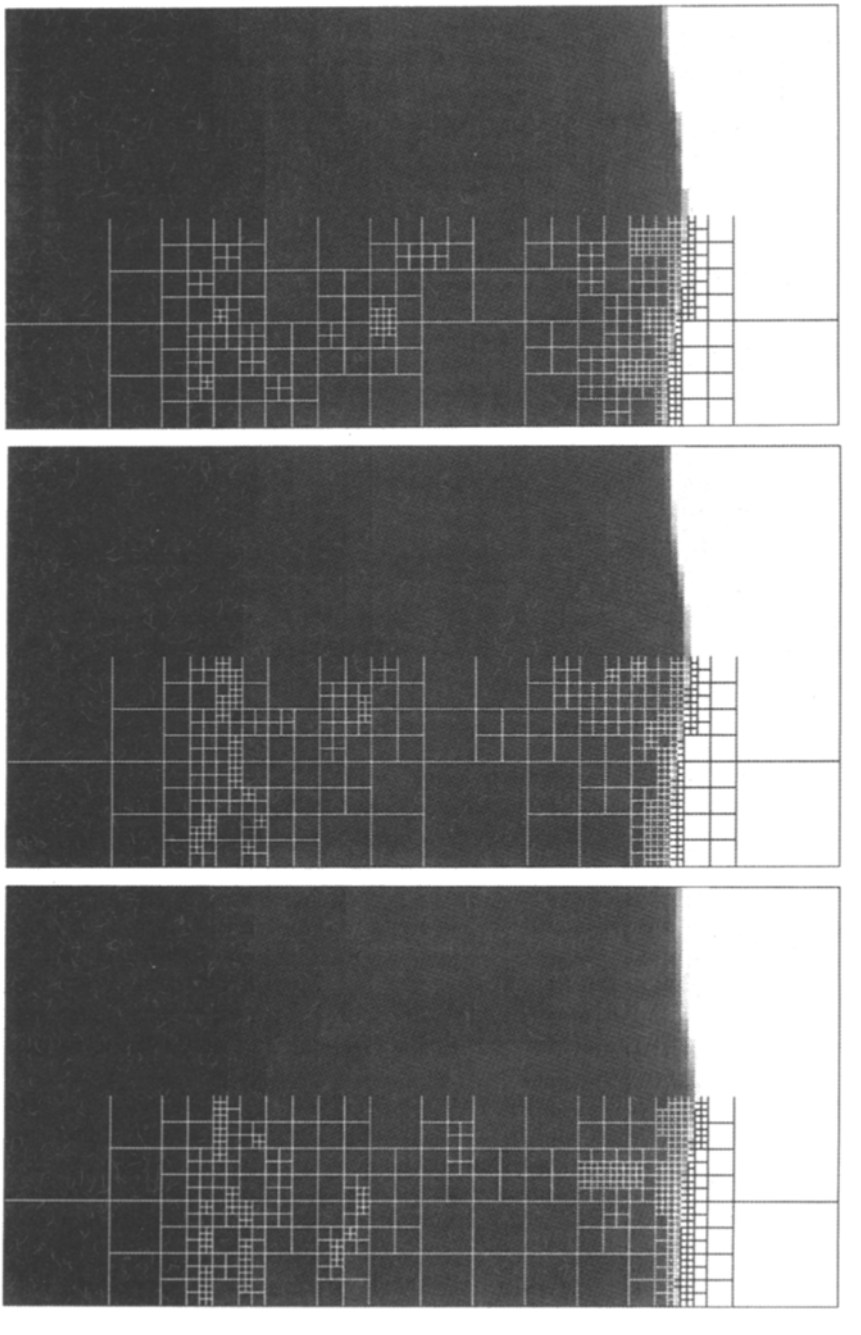

Fig. 2. Solution of the inflow/outflow problem for a stable displacement process with no capillary pressure using, from top to bottom, 32, 64, and 128 time steps.

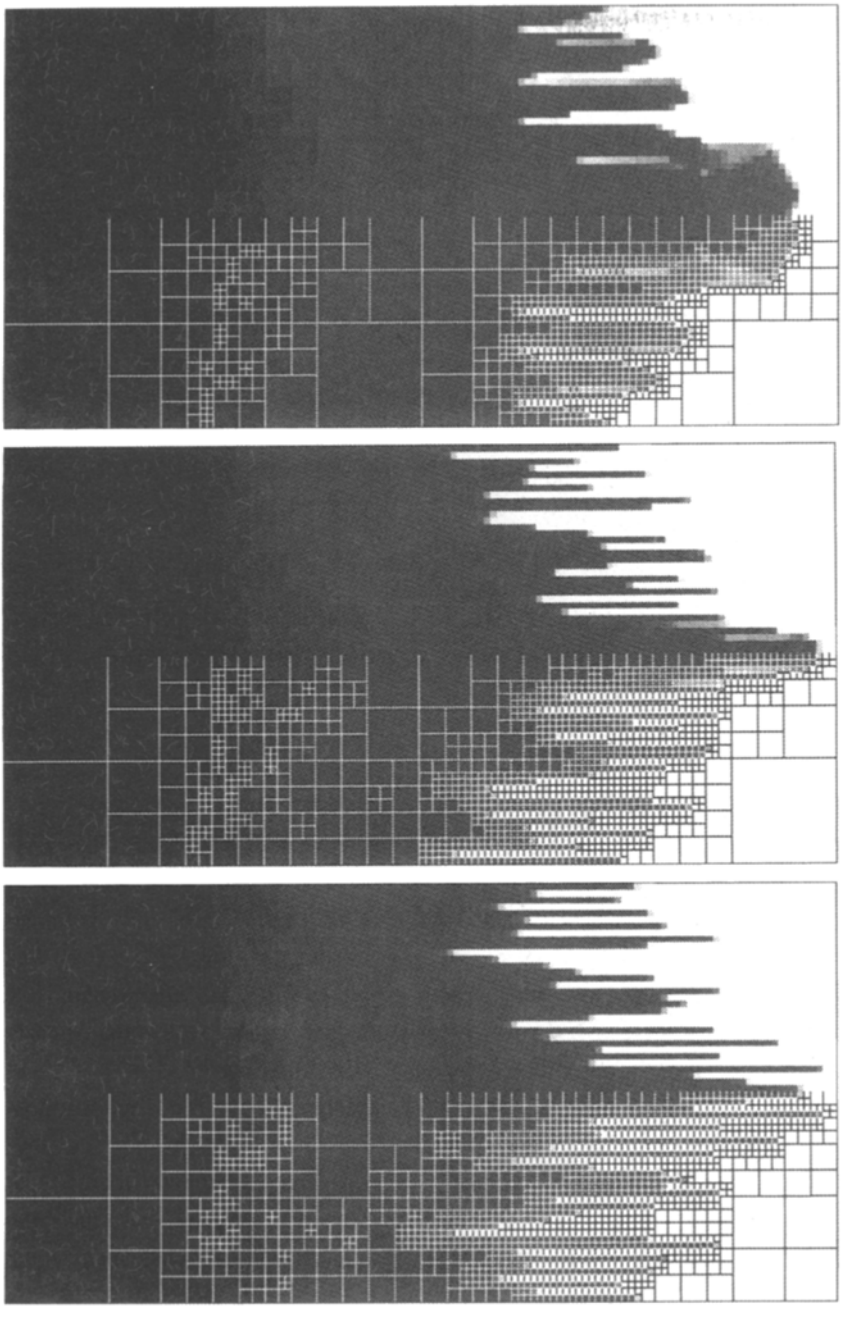

Fig. 3. Solution of the inflow/outflow problem for an unstable displacement process with no capillary pressure using, from top to bottom, 32, 64, and 128 time steps.

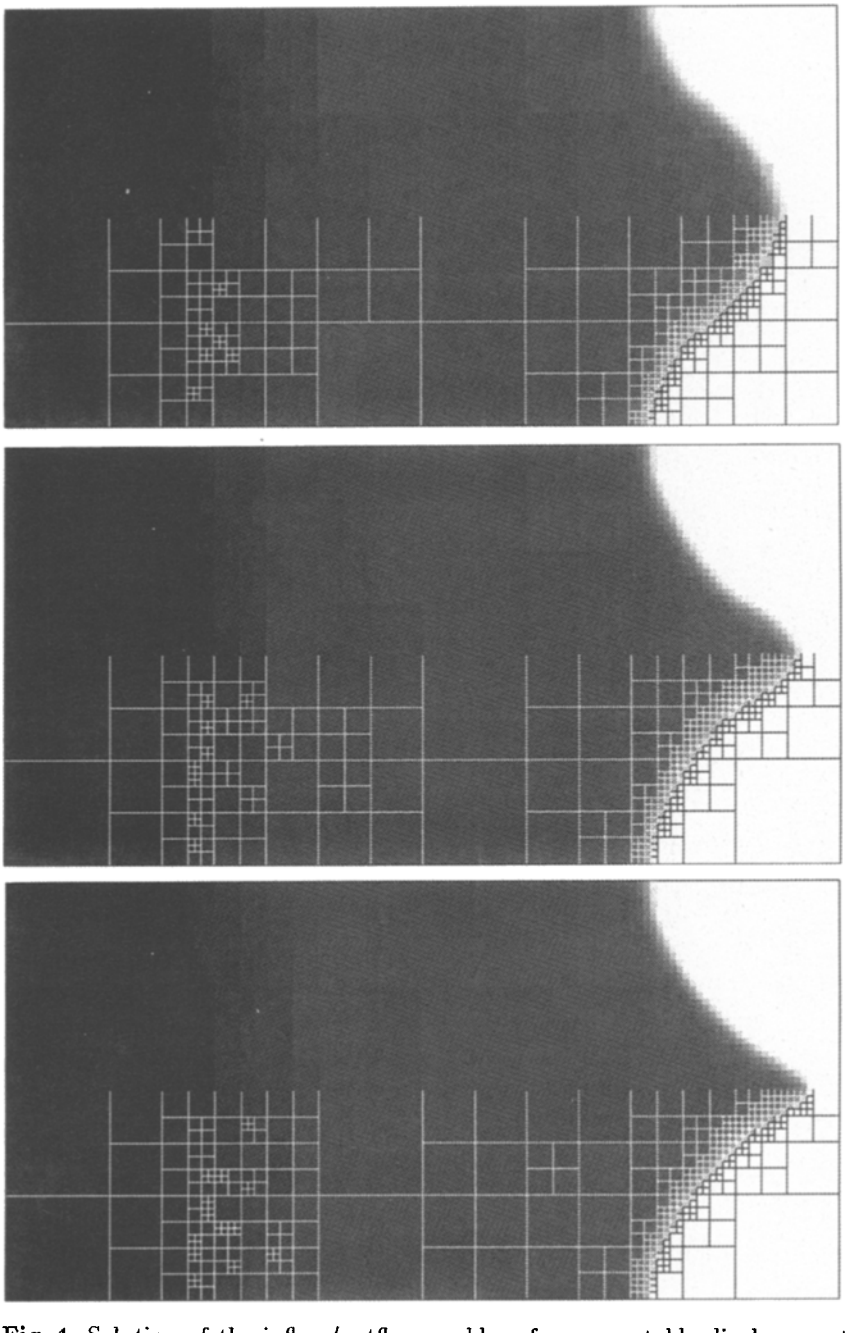

Fig. 4. Solution of the inflow/outflow problem for an unstable displacement process including capillary pressure using, from top to bottom, 32, 64, and 128 time steps.

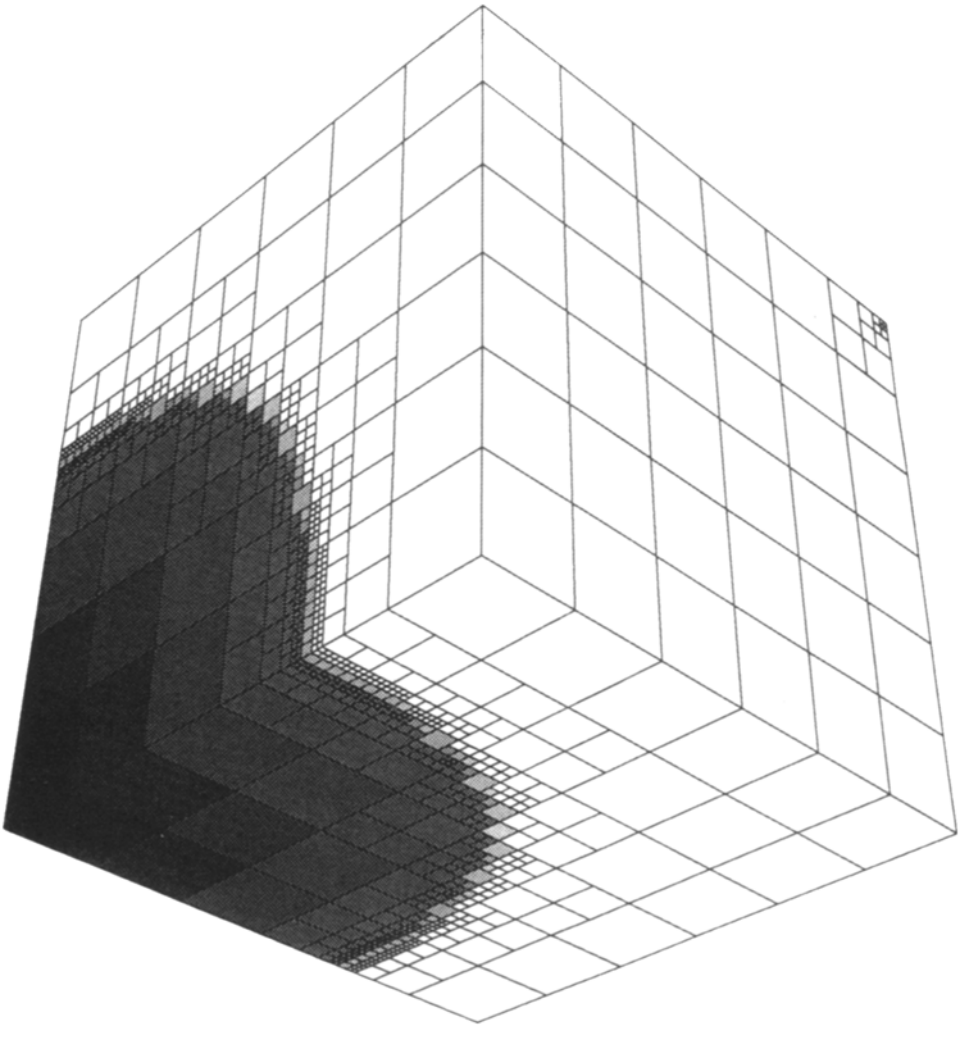

Fig. 5. Solution of the three-dimensional equivalent of the quarter-five-spot problem at 0.15 PVI using only one time step.

This article was processed using the LaTeX macro package with ICM style